VSC-TR-83-3

NONLINEAR MODELING OF TECTONIC RELEASE FROM UNDERGROUND EXPLOSIONS

S. M. Day
J. T. Cherry
N. Rimer
J. L. Stevens

S-CUBED
P. O. Box 1620
La Jolla, California 92038

TOPICAL REPORT

August 1982

Monitored by:

VELA Seismological Center
312 Montgomery Street
Alexandria, Virginia 22314

Unclassified

SECURITY CLASSIFICATION OF THIS PAGE (When Data Entered)

REPORT DOCUMENTATION PAGE

READ INSTRUCTIONS BEFORE COMPLETING FORM

1. REPORT NUMBER: VSC-TR-83-3	2. GOVT ACCESSION NO.: AD-A116051
3. RECIPIENT'S CATALOG NUMBER:	
4. TITLE (and Subtitle): Nonlinear Modeling of Tectonic Release from Underground Explosions	5. TYPE OF REPORT & PERIOD COVERED: Topical Report
	6. PERFORMING ORG. REPORT NUMBER: SSS-R-82-5555
7. AUTHOR(s): S. M. Day, J. T. Cherry, N. Rimer, and J. L. Stevens	8. CONTRACT OR GRANT NUMBER(s): F08606-79-C-0008
9. PERFORMING ORGANIZATION NAME AND ADDRESS: S-CUBED, P. O. Box 1620, La Jolla, California 92038	10. PROGRAM ELEMENT, PROJECT, TASK AREA & WORK UNIT NUMBERS: ARPA Order No. 4436
11. CONTROLLING OFFICE NAME AND ADDRESS:	12. REPORT DATE: August 1982
	13. NUMBER OF PAGES: 35
14. MONITORING AGENCY NAME & ADDRESS (if different from Controlling Office): VELA Seismological Center, 312 Montgomery Street, Alexandria, Virginia 22314	15. SECURITY CLASS. (of this report): Unclassified
	15a. DECLASSIFICATION/DOWNGRADING SCHEDULE:

16. DISTRIBUTION STATEMENT (of this Report)

Approved for Public Release, Distribution Unlimited.

17. DISTRIBUTION STATEMENT (of the abstract entered in Block 20, if different from Report)

18. SUPPLEMENTARY NOTES

19. KEY WORDS (Continue on reverse side if necessary and identify by block number)

Tectonic Release
Rayleigh Waves
Numerical Simulation
Synthetic Seismograms
Nonlinear
Phase Reversal

20. ABSTRACT (Continue on reverse side if necessary and identify by block number)

Reversal of teleseismic Rayleigh wave polarity has been observed for some underground explosions in eastern Kazakh, and in some cases the polarity is reversed at all azimuths of observation. We analyze two-dimensional, nonlinear numerical simulations of underground explosions to examine the hypothesis that these phase reversals result from the action of tectonic prestress on the explosion-created nonlinear volume. We conclude that the effect of tectonic prestress on surface wave excitation is potentially large.

cont A

DD FORM 1 JAN 73 1473 EDITION OF 1 NOV 65 IS OBSOLETE

Unclassified

SECURITY CLASSIFICATION OF THIS PAGE (When Data Entered)

When a shear prestress of 7.5 MPa (75 bars) is introduced, with horizontal principal stresses more compressive than the vertical principal stress, the explosion Rayleigh wave amplitude is reduced by a factor of 4 (i.e., M_S is reduced by 0.6). The large surface wave reduction is accompanied by no significant perturbation of the body wave magnitude (m_b). The nonlinear model predictions imply that if tectonic release is modeled elastically as the relaxation of the deviatoric part of the prestress into a spherical cavity, the appropriate cavity radius is approximately 80 percent of the explosion elastic radius.

Assuming that the explosion and tectonic release components of the source add linearly, i.e., assuming the surface wave reduction is proportional to the deviatoric prestress, then tectonic shear stress exceeding 10 MPa (100 bars) would be sufficient to reverse the Rayleigh wave polarity. Shear stresses of this magnitude are plausible at several hundred meters depth, in that they do not exceed strength bounds for a fractured rock mass, as estimated from Byerlee's law. Therefore, this hypothesis should be tested through further two-dimensional nonlinear modeling at higher prestress levels.

AFTAC Project Authorization No. VT/0712/B/PMP
ARPA Order No. 4436
Effective Date of Contract: November 17, 1978
Contract Expiration Date: November 15, 1981
Amount of Contract: $1,816,437
Contract No. F08606-79-C-0008
Principal Investigator and Phone No.
Dr. J. Theodore Cherry, (619) 453-0060
Project Scientist and Phone No.
Mr. Brian W. Barker, (202) 325-7581

This research was supported by the Advanced Research Projects Agency of the Department of Defense and was monitored by AFTAC/VSC, Patrick Air Force Base, Florida 32925, Under Contract No. F08606-79-C-0008.

W/O 11098

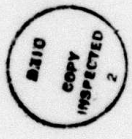

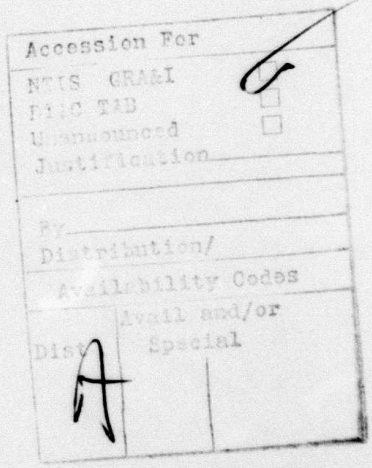

TABLE OF CONTENTS

LIST OF ILLUSTRATIONS

LIST OF TABLES

I. INTRODUCTION

It has long been recognized that spherically symmetric source representations do not account for important aspects of the body and surface waves radiated by underground explosions. Nonisotropic components of the explosion source can even be sufficiently strong, in some cases, to reverse the polarity of the teleseismic Rayleigh wave at some azimuths. This phenomenon has been observed for some NTS events, as described by, for example, Toksoz and Kehrer (1971). A number of investigators have recently noted reversed-polarity Rayleigh waves from some events in eastern Kazakhstan, and in some of these cases the polarity is reversed at all azimuths of observation (e.g., Rygg, 1979; Patton, 1980; Cleary, 1981). It is not known what concomitant effect the nonisotropic source component has on the body wave radiation from these explosions.

The present work is motivated by the need to understand the dominant physical processes causing the anomalous surface wave radiation. Such understanding is important for obtaining reliable seismic estimates of explosion yield.

Several mechanisms have been proposed to explain anomalous radiation from underground explosions, and these have been recently reviewed by Masse (1981). They include spallation, explosion-triggered tectonic earthquakes, explosion-driven passive slip on faults, and release of tectonic prestress within the explosion source volume. In a previous report (Day, Rimer and Cherry, 1982) we used analytical and numerical source models to argue that spall does not significantly modify the long-period surface wave radiation from underground explosions and therefore cannot induce Rayleigh wave polarity reversals.

In this report, we examine the tectonic stress release mechanism. By tectonic release, we will mean relaxation of the tectonic prestress field around the explosion-created nonlinear zone surrounding the working point. We distinguish this hypothesis from the hypothesis of earthquake triggering on faults outside the

immediate vicinity of the working point (e.g. Aki and Tsai, 1972). We address particularly the question of whether tectonic prestress is a potential explanation for observations of reverse-polarity Rayleigh waves. The basis for our analysis is a pair of two-dimensional (axisymmetric), nonlinear simulations of an explosion in granite. In one case, the prestress is hydrostatic, and in the second case a deviatoric component is added, representing a tectonic load. We quantify the effect of tectonic prestress on the seismic radiation by comparing teleseismic body and surface wave predictions from the two simulations. Analysis of a third model, a one-dimensional (spherically symmetric) simulation in a uniformly, hydrostatically prestressed wholespace, provides a strong check on the analysis procedures.

The linear theory of tectonic release due to the weakened zone around an explosion source has been extensively developed over the past two decades (e.g., Press and Archambeau, 1962; Archambeau and Sammis, 1970; Archambeau, 1972; Minster, 1973; Stevens, 1980a). In these studies, the tectonic component of the source has been modeled elastically as the relaxation of a prestress field around a spherical cavity. Analytic solutions have been obtained for both uniform and nonuniform applied stresses (Stevens, 1980a). The seismic radiation from the tectonic release model can be superposed on that for a spherically symmetric explosion source model to predict the seismic signal. This model provides a linear approximation to the complex nonlinear processes associated with an explosion in a prestressed medium.

The main source of uncertainty in the linear model is that there is no firm physical basis from which to determine the "equivalent" cavity radius -- that is, the radius of a spherical cavity which will simulate the effect of the explosion nonlinearities. The actual explosion cavity radius is a lower bound, while the explosion elastic radius provides an upper bound. However, this leaves an order of magnitude uncertainty in the equivalent cavity radius. Since the amplitude of long-period

seismic radiation from the linear model is proportional to the cube of this radius, we are left with a very large uncertainty in the surface wave excitation from this model.

A second source of uncertainty in the linear model is the possibility that the prestress field may itself significantly perturb the nonlinear behavior of the near-source material. Therefore there is doubt about the adequacy of linearly superposing monopole and tectonic release components to estimate the seismic radiation as a function of prestress level.

The nonlinear simulations analyzed in this report show that the effect of tectonic prestress on surface wave amplitudes is potentially large. When a shear prestress of 7.5 MPa (75 bars) is introduced, with horizontal principal stresses more compressive than the vertical principal stress, the explosion Rayleigh wave amplitude is reduced by a factor of four. Furthermore, this large surface wave reduction is accompanied by no significant change in body wave magnitude. In this case, comparison with the linear theory gives an equivalent cavity radius for tectonic release equal to approximately 80 percent of the elastic radius of the explosion.

If we assume that the tectonic release component adds linearly to the explosion radiation, in proportion to the prestress level, then our numerical results imply that a shear prestress exceeding 10 MPa (100 bars) would be sufficient to reverse the Rayleigh wave polarity. This hypothesis needs to be investigated through further nonlinear modeling.

II. THE EXPLOSION MODELS

2.1 INTRODUCTION

To investigate the seismic radiation due to the action of tectonic stresses on the zone of failure around an underground explosion, we make use of numerical simulations, which can incorporate models of nonlinear material response. Previously, most such modeling of explosions has been done in one dimension. For example, extensive use has been made of the finite difference method in one dimension for studying spherically symmetric explosion sources (e.g., Cherry et al. 1975; Bache et al. 1975). This work has focused on the so-called "seismic coupling" problem, that is, the dependence of the radiated seismic wavefield on near-source material properties.

Simulations including nonlinear interaction with the free surface, such as spall, require two-dimensional (axisymmetric) numerical methods. For example, Day, Rimer and Cherry (1982) used two-dimensional finite difference simulations of explosions in granite to study the effect of spall on the Rayleigh waves from buried explosions. In this report, we use two-dimensional simulations to study the effect of tectonic prestress on the explosion radiation field.

A pair of two-dimensional simulations of a buried explosion in granite were performed using a finite difference method. In both cases, the source-region geologic structure was a three-layered halfspace representing the geology at the site of the 1966 PILEDRIVER explosion at the Nevada Test Site (NTS), as described by Rimer, et al. (1979). The nonlinear material model used in the calculations is also described by Rimer, et al., and includes tensile failure, shear failure, irreversible pore collapse, and an effective stress law. The explosion depth and yield were the same as for PILEDRIVER, 463 meters and 61 KT, respectively. A one-dimensional (spherically symmetric) explosion simulation was also performed for comparison to the two-dimensional source models.

2 2 CASE 1: ONE-DIMENSIONAL MODEL

In this numerical simulation, gravity and free surface effects were neglected, and the prestress was assumed to be isotropic and uniform. This simulation was performed using the same nonlinear constitutive model as was used for the two-dimensional simulations; the P and S wave velocities and density were 5350 m/sec, 2790 m/sec, and 2650 kg/m^3, respectively. The prestress value corresponded to the overburden at shot depth (12 MPa at 463 meters).

An equivalent elastic point source for the one-dimensional model consists of a center of dilatation with a time history given by the reduced displacement potential (RDP) time history of the explosion, which is readily computed from the one-dimensional simulation. Synthetic seismograms at teleseismic range can be computed from this equivalent point source. We will find that this computation provides a very strong validation of the more complex method used to compute teleseismic radiation from the two-dimensional simulations. The spectrum of the reduced velocity potential (time derivative of the RDP) for the one-dimensional model is shown in Figure 1. Its low frequency limit (i.e., the static level of the RDP), denoted by Ψ_∞, is $1.6 \times 10^4 m^3$.

2.3 CASE 2: TWO-DIMENSIONAL HYDROSTATIC MODEL

In the first two-dimensional simulation, the prestress is assumed to result from overburden only and to be hydrostatic. The results of this explosion simulation have been summarized by Day, Rimer and Cherry (1982). Figure 2, taken from that paper, shows computed vertical velocity time histories in the near-field and compares these with recorded ground velocities for PILEDRIVER (from Hoffman and Sauer, 1969). Spall occurs at all the sites, immediately after the first velocity peak, as evidenced by the -1 g slopes of the velocity waveforms. Spall closure can be identified with the termination of the -1 g slope. From the figure, we can see that the simulation somewhat over-predicts the initial spall velocity, and therefore the ballistic period. This is especially

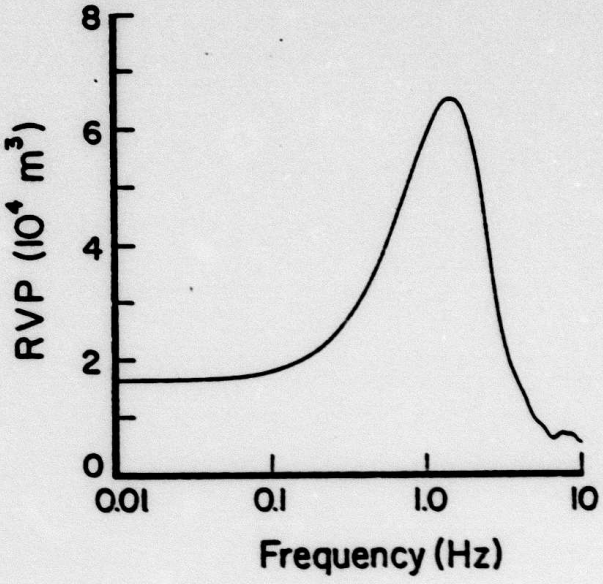

Figure 1. The reduced velocity potential (RVP) spectrum for the one-dimensional simulation of a 61KT explosion in granite.

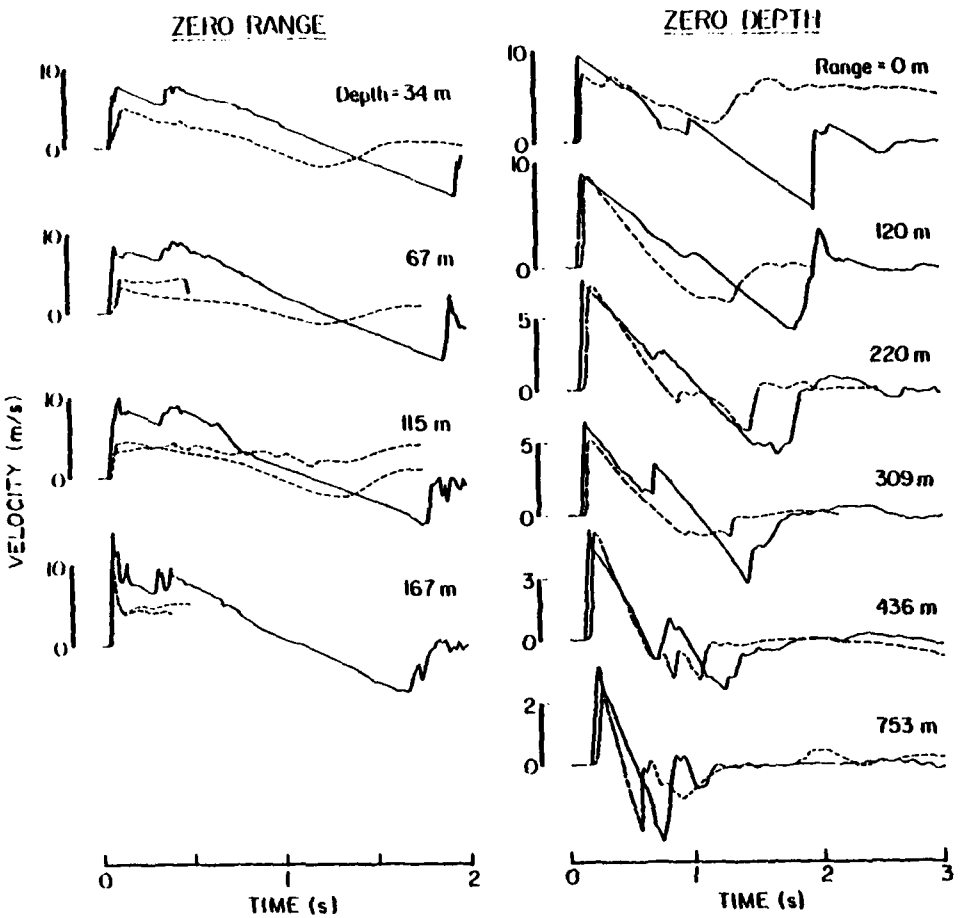

Figure 2. Vertical velocity time-histories (positive up) obtained from the two-dimensional simulation (Case 2), compared with recorded velocities for PILEDRIVER. The data are from Hoffman and Sauer (1969). Occurrence of spall is apparent from the -1 g slopes in the velocity waveforms.

noticeable near ground zero, less so at large range. The representative ballistic period near ground zero, for the simulation, appears to be about 1.7 seconds, compared to the observed period for PILEDRIVER which appears to be about 1.2 seconds. The simulation replicates very well the decrease of ballistic period with increasing range, as well as the decay of peak particle velocity. Overall, the simulation represents the main features of the PILEDRIVER recordings fairly well.

Our next step is to introduce a nonhydrostatic component into the initial stress field. Then the teleseismic body and surface wave radiation for the three cases will be compared.

2.4 CASE 3: TWO-DIMENSIONAL TECTONIC MODEL

The second two-dimensional simulation differs from the first only in that a nonhydrostatic initial stress is added to the medium. We assume that the vertical prinicipal stress is equal to the overburden, and that the two horizontal principal stresses are equal to each other and larger (more compressive) than the vertical principal stress (see Figure 3). We choose the horizontal principal stress to exceed the vertical principal stress because we are interested in explaining observations of reversed-polarity Rayleigh waves; the Rayleigh wave radiated by relaxation of a stress field with this orientation will tend to oppose the Rayleigh wave radiated by an explosive monopole (see, for example, Harkrider, 1981). Equality of the two horizontal principle stresses insures that cylindrical symmetry is preserved, so we can use the two-dimensional numerical method used in Case 2.

The next problem is to estimate a plausible level of tectonic shear stress at depths of a few hundred meters. Brace and Kohlstedt (1980) propose that Byerlee's law be used as a basis for estimating an upper bound on shear stress as a function of depth. Byerlee (1968) noted that frictional resistance of rock fractures is nearly independent of rock type. For effective normal stress $\tilde{\sigma}_n$ (i.e., compressive normal stress on the fracture, minus pore fluid

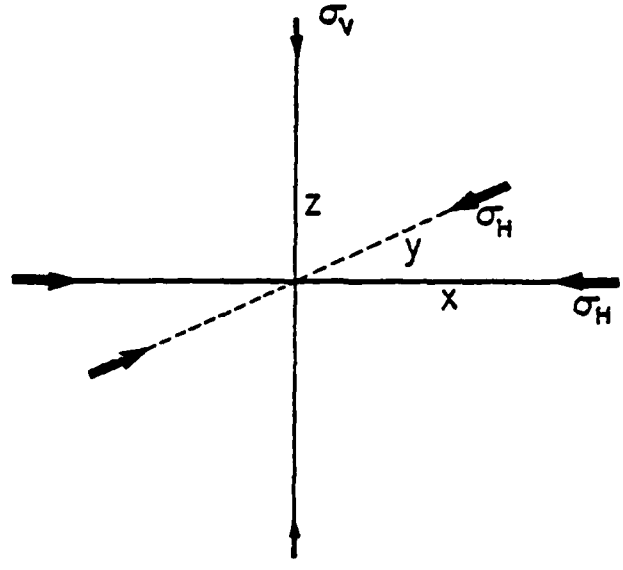

Prestress orientation

horizontal principal stress (σ_H)	>	vertical principal (σ_V) stress

Figure 3. Orientation of the stress field for Case 3. The horizontal principal stresses are equal, and are more compressive than the vertical principal stress.

pressure) up to about 200 MPa, Byerlee's relationship for the maximum frictional stress, τ, is

$$\tau \approx 0.85\,\tilde{\sigma}_n \quad . \tag{1}$$

(Byerlee, 1978). Following Brace and Kohlstedt (also see Jaeger and Cook, 1976, p. 14), we express Byerlee's law in terms of the maximum and minimum principal effective stresses $\tilde{\sigma}_1$ and $\tilde{\sigma}_3$, respectively:

$$\tilde{\sigma}_1 \approx 5\,\tilde{\sigma}_3 \tag{2}$$

If fractures of all orientations exist, and σ_3 is vertical and equal to the overburden, then Equation (2) yields a bound on the maximum stress difference. Assuming hydrostatic pore pressure, with the density of water equal to 40 percent of the rock density, (2) gives the following result:

$$(\sigma_1 - \sigma_3) \lesssim 2.4\,\rho g h, \tag{3}$$

where ρ is the rock density, g is the gravitational acceleration, and h is the depth. This bound on the stress difference is about 30 MPa at working point depth, giving a maximum shear stress (that is, one half the stress difference) of about 15 MPa. For dry rock (zero pore pressure), the bounds estimated in this manner would be about 60 percent higher.

McGarr and Gay (1978) reviewed in situ stress measurements made in North America, Southern Africa, Central Europe, Australia, and Iceland. These data generally support the assumption that the vertical principal stress is approximately given by the weight of the overburden. McGarr and Gay also found that maximum shear stress determinations at between 100 and 1000 meters depth tend to be significantly lower than those at greater depth. The shallow data scatter between about 0 and 15 MPa. More recently, Zoback, Tsukahara, and Hickman (1980) measured in situ stress in wells drilled near the San Andreas fault and obtained the vertical and

horizontal profiles shown in Figure 4. In the Western Mojave desert, at a distance of 4 km from the San Andreas, they find that shear stress increases from about 2.5 MPa at 150-300 meters depth to about 8 MPa at 750-850 meters depth.

In light of these observations, we have set the horizontal principal stresses in our simulation to vary with depth so as to give the maximum shear stress profile shown as a solid curve in Figure 5a. The maximum shear stress is uniform at 7.5 MPa for depths greater than 320 meters, and tapers to zero at 140 meters depth. This level is well below the bound estimated from Byerlee's law, which is shown as a dashed line in the Figure 5a.

Figure 5b compares the inelastic volume determined from the numerical simulation of Case 3 (tectonically prestressed) with the inelastic volume of Case 2 (hydrostatically prestressed). The final cavity volumes in Cases 2 and 3 are nearly identical. The radial extent of inelastic response is slightly less for Case 3 than for Case 2. This is a consequency of the increased horizontal load in Case 3 compared with Case 2. Increasing the horizontal load also increases the confining pressure. In these simulations (and all numerical explosion simulations for low-porosity rock which we have studied), shear failure near the periphery of the nonlinear zone occurs during unloading of the medium into a tensile state. Thus, the elevated confining pressure in Case 3 tends to inhibit failure and therefore reduces the size of the of the inelastic volume.

For Case 1, the inelastic volume is spherical and can be described by an elastic radius. In this simulation the elastic radius, which is indicated in Figure 5b, is 598 m.

For a source which is not spherically symmetric, of course, the nonlinear volume is not so easily characterized. In the two-dimensional simulations, the maximum range at which inelastic response occurs depends on depth. For depths shallower than about 150 meters, in fact, nonlinearities persist out to a radius of 1000 meters, beyond which nonlinearity was artificially suppressed in the calculations. This near-surface nonlinearity is the result of spall

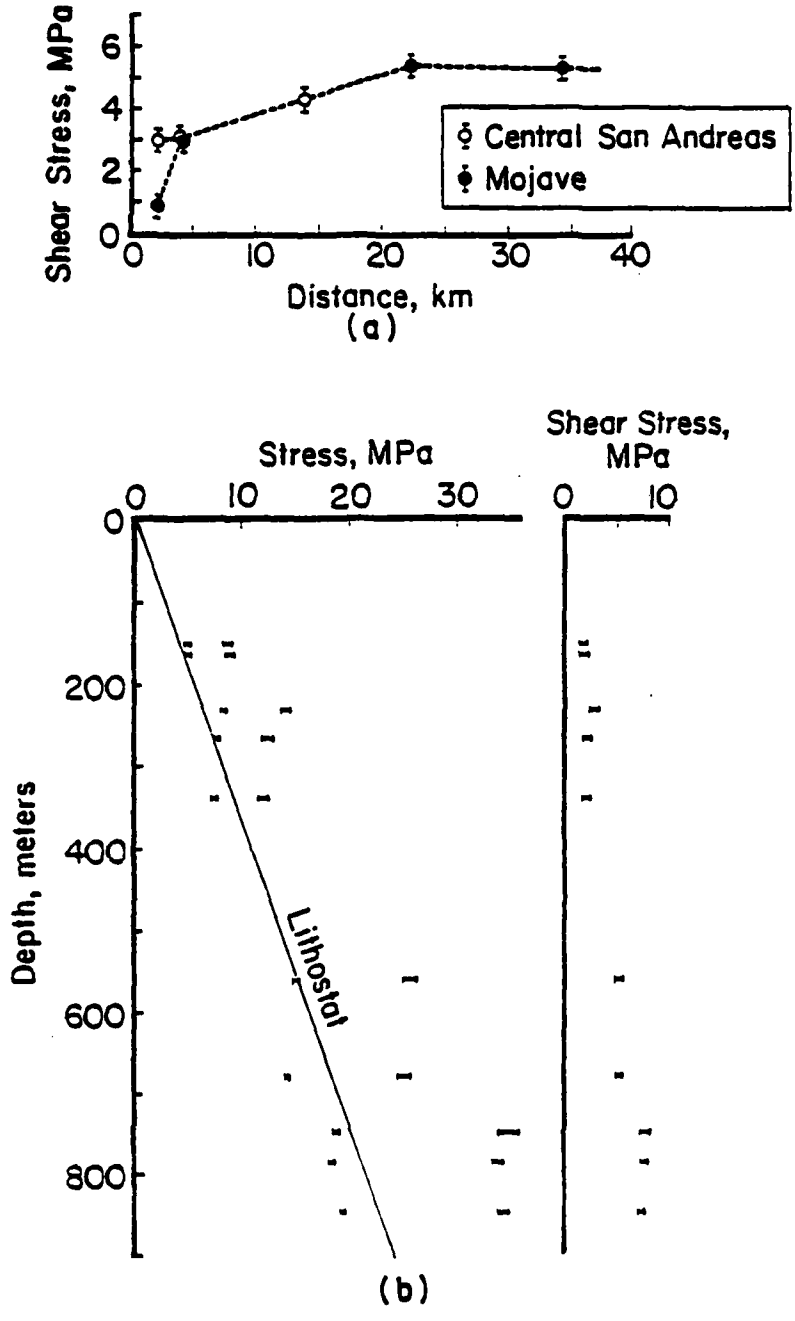

Figure 4. (a) Shear stress at a depth of 200 meters, as a function of distance from the San Andreas fault (from Zoback et al., 1980).

(b) Horizontal principal stresses and shear stress as a function of depth, measured at a distance of 4 km from the San Andreas fault.

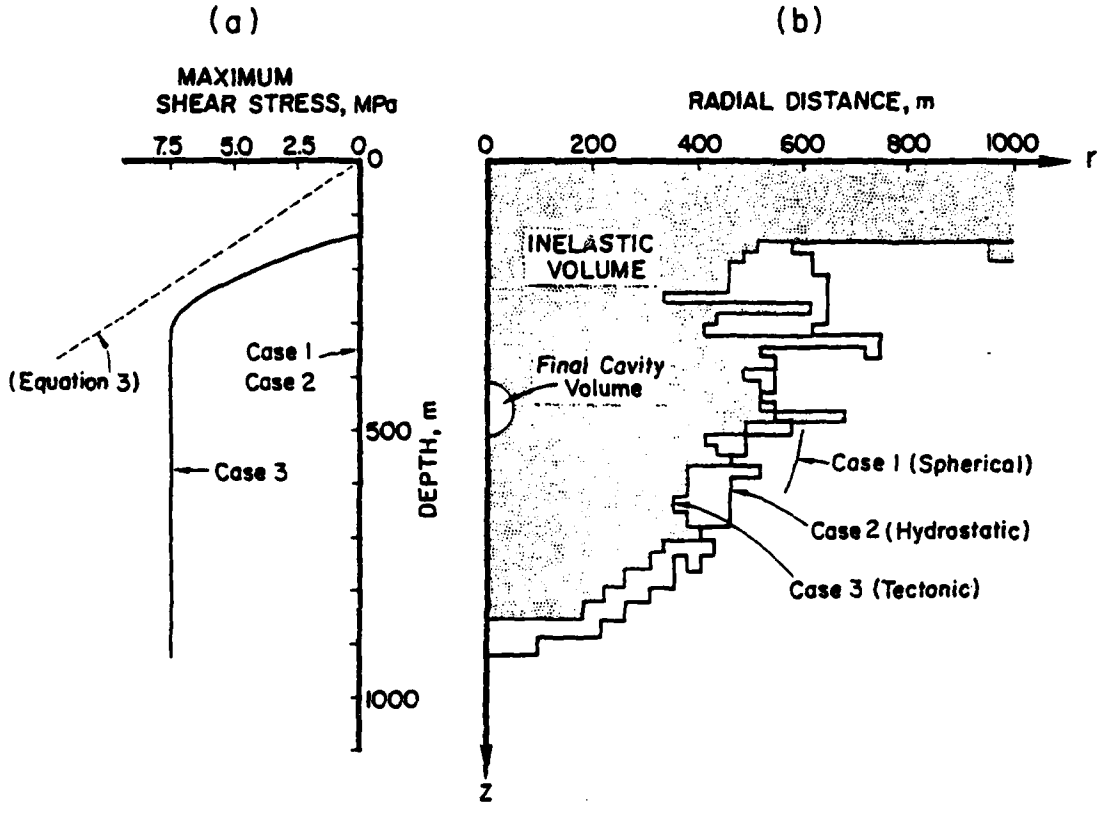

Figure 5. (a) Initial shear stress for the numerical simulations. The solid curve is the maximum shear stress as a function of depth, for Case 3 (for Cases 1 and 2 the initial shear stress was zero). The dashed line is the upper bound as estimated from Equation 3.

(b) The inelastic volume obtained for the three simulations. In the two-dimensional simulations, nonlinear material response was artificially suppressed beyond a range of 1000 m. The final explosion cavities for Cases 2 and 3 are indistinguishable (the explosion cavity for Case 1, not shown, had a radius approximately 15% smaller).

of the surface material, and is consistent with the fact that spall is observed out to several kilometers range from many underground tests. Below the spall layer, the inelastic range at shot depth can be taken as a representative value of the "elastic radius." In both Case 2 and Case 3, this range is about 550 meters.

In the next section, we present synthetic Rayleigh wave seismograms for the one-dimensional and two-dimensional simulations. These synthetic seismograms are compared in order to quantify the perturbation to the surface wave radiation which is attributable to tectonic loading. A subsequent section then compares short-period teleseismic P-wave synthetics from the three simulations, in order to predict the accompanying effects on body wave magnitude measurements.

III. RAYLEIGH WAVES

We compute the fundamental mode teleseismic Rayleigh waves from the two-dimensional simulations described in the last chapter, using the method of Bache, Day and Swanger (1982). This procedure uses the representation theorem (e.g., Burridge and Knopoff, 1964) to compute the teleseismic radiation by means of a surface integral of the near-source displacements and tractions. These are evaluated on a closed surface surrounding the nonlinear source region (Figure 6). In this case, the surface of integration was a cylinder with radius and depth of 1209 meters.

As shown by Day, Rimer and Cherry (1982), any failure of the near-source solution to conserve momentum will lead to a long-period error in the surface wave prediction by this method. To verify that the finite difference simulations conserve momentum to sufficient precision for purposes of computing teleseismic surface waves, we plot in Figure 7 the total vertical momentum enclosed by the intergration cylinder (Σ), as a function of time, for Case 2 and Case 3, respectively. Also plotted on the figure is the time integral of the total vertical force (total impulse) exerted on Σ by the exterior continuum in each case. In this figure, force is taken relative to its initial equilibrium value (i.e., the prestresses have been subtracted). In the absence of numerical errors, the momentum and impulse curves should coincide and should approach zero at late time. The agreement shown in Figure 7 is very satisfactory; the slight tendency for the momentum curve to lead the impulse curve is a result of the causal low-pass filtering and decimation to which the stress time histories were subjected prior to integration over Σ.

The results in Figure 7 give us added confidence that we can accurately compute long-period synthetic seismograms for the two-dimensional simulations using the representation theorem. This we do using the three-layered earth structure given in Table 1. Fundamental mode Rayleigh wave synthetic seismograms were computed at 3000 km range, with the long-period LRSM seismometer response included.

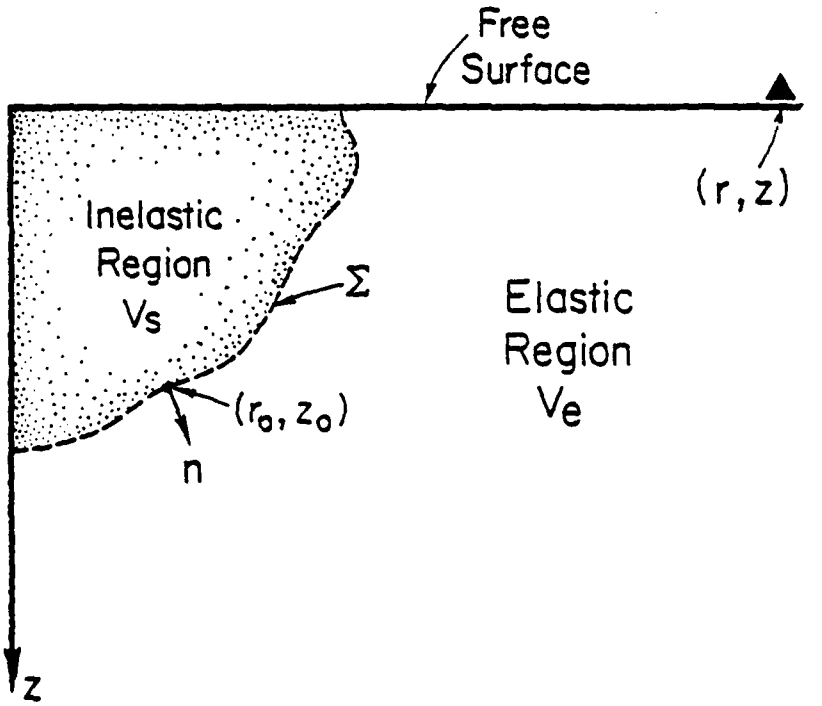

Figure 6. Geometry for the surface-integral representation of the seismic radiation from an axisymmetric explosion source. The receiver point is (r,z), and a typical point lying on the imaginary surface Σ is (r_0,z_0). The surface Σ lies wholly outside the nonlinear region surrounding the source.

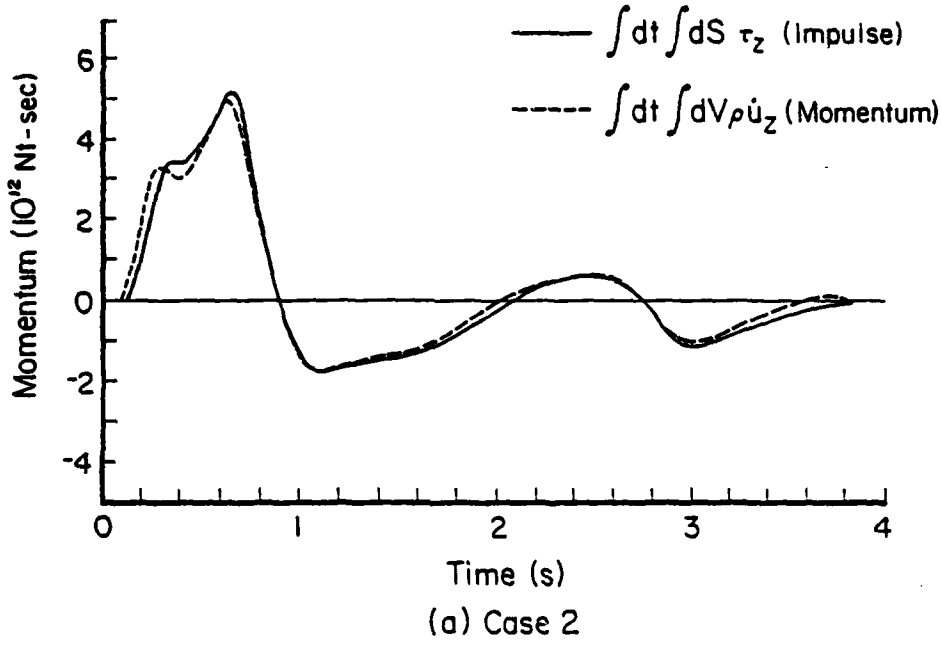

(a) Case 2

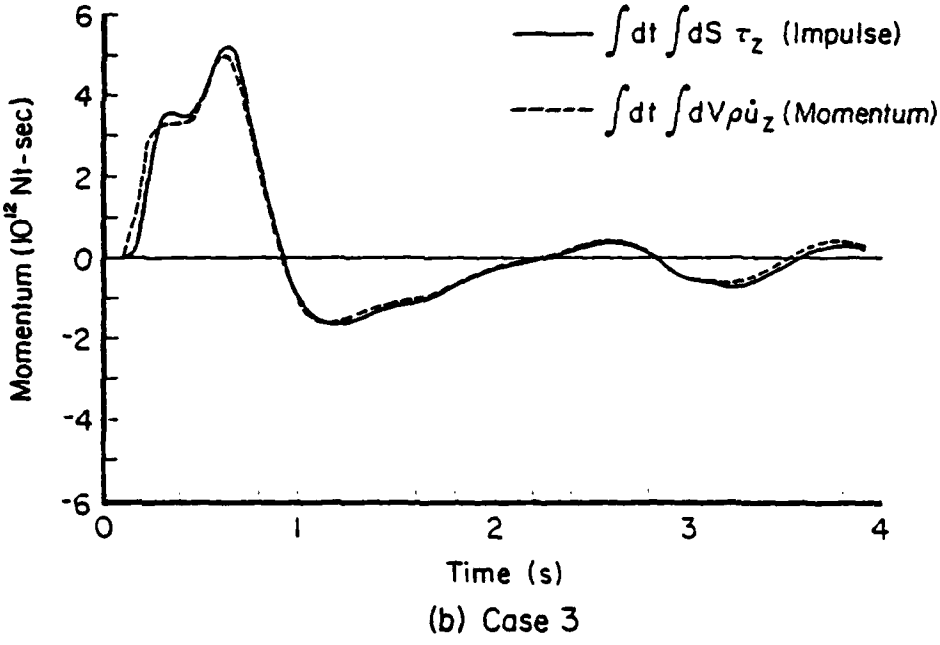

(b) Case 3

Figure 7. Total momentum (positive up) in the source volume, V_s, compared with the total impulse on its boundary, Σ, for the two-dimensional explosion simulations: (a) Case 2 and (b) Case 3. In each case, the fact that the curves are nearly coincident and approach zero at late time demonstrates that the computation properly conserves momentum.

TABLE 1

PROPAGATION PATH MODEL FOR THE
RAYLEIGH WAVE SYNTHETIC SEISMOGRAMS

Layer Thickness (km)	α (m/sec)	β (m/sec)	ρ (kg/m^3)	Q_β
25	5500	3180	2650	200
20	6400	3700	2900	500
	8100	4680	3500	1000

Figure 8 shows the synthetic seismograms for all three two-dimensional simulations, as well as for the one-dimensional simulations. The waveform for Case 1 (the one-dimensional simulation) is indistinguishable from that of Case 2 (the two-dimensional hydrostatic case). Furthermore, there is no discernible time delay between the seismograms and the peak-to-peak amplitudes agree to within less than half of one percent. This result was discussed by Day, Rimer and Cherry (1982). Combined with analytical results derived therein, this comparison constitutes strong evidence that spall cannot produce significant amplitude or phase anomalies in long-period surface wave radiation. Moreover, the extremely precise agreement between these one- and two-dimensional simulations is very strong corroboration of the accuracy with which the long-period radiation has been computed by the representation-theorem integral.

Comparing Case 2 with Case 3 in Figure 8, however, we find that the introduction of tectonic prestress appreciably perturbs the long-period Rayleigh waveform and greatly reduces its amplitude. Maximum peak-to-peak amplitude for Case 3 is a factor of 4.12 lower than for Case 2. This is a surface wave magnitude (M_s) reduction of about 0.6 units compared to the hydrostatic case. In addition to having a greatly reduced amplitude, the tectonic release model also shows a small time delay (about one second) of the peak amplitude arrival in the Rayleigh wave train. There is no polarity reversal, however.

The amplitude comparisons in Figure 8 serve to quantify the effect of tectonic release on long-period Rayleigh wave excitation, as estimated from the nonlinear simulations. We now compare these results from the nonlinear source models with a linear model of tectonic release.

The linear theory (e.g., Archambeau and Sammis, 1970) assumes that nonlinear deformation reduces the resistance to shear of the material around the explosion, and that the dynamic effects of

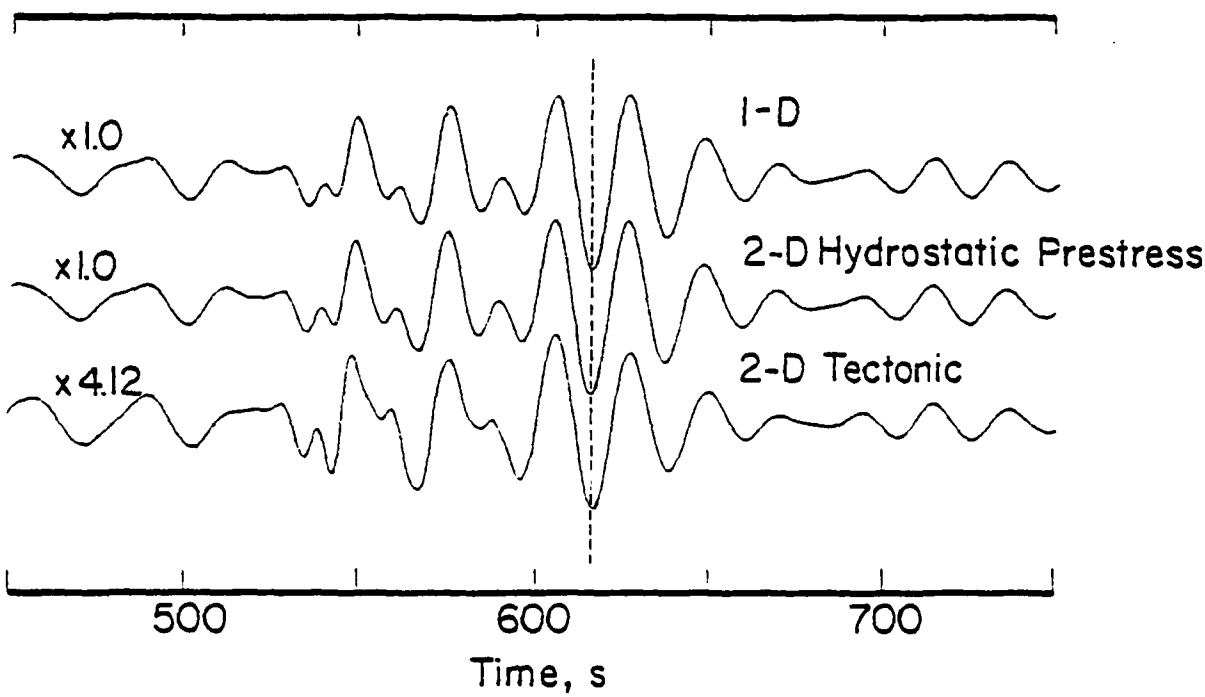

Figure 8. Synthetic fundamental-mode Rayleigh waves for the one- and two-dimensional explosion simulations, compared at a range of 3000 km. Under hydrostatic prestress, two-dimensional effects, including spall, have had no perceptible effect on the amplitude or waveform. Introduction of tectonic prestress, however, has perturbed the long-period waveform and reduced the maximum peak-to-peak amplitude by more than a factor of 4.

tectonic stresses acting on this zone can be approximately represented by the sudden introduction of a cavity into a linearly elastic, prestressed continuum. The nonlinear simulations afford a means of calibrating the linear theory. In particular, we will estimate an equivalent cavity radius — that is, the radius of a spherical cavity which, in the linear theory, would simulate the nonisotropic seismic effect of the explosion nonlinearities. (This equivalent cavity radius, R, is not to be confused with the actual cavity radius of the explosion, nor with the explosion elastic radius.)

Stevens (1980a) gives a general solution for the seismic radiation from the relaxation of a prestress field into a spherical cavity in a homogenous, linearly elastic wholespace. In the long period limit, which is appropriate for teleseismic surface waves, this tectonic release model can be given a point source description in terms of a moment tensor. As shown in the appendix, the moment tensor describing tectonic release has components M_{ij} given by

$$M_{ij} = \sigma'_{ij} R^3 \frac{20\pi\alpha^2}{9\alpha^2 - 4\beta^2} , \tag{3}$$

where σ_{ij} is a component of the deviatoric part of the prestress tensor, R in the cavity radius, and α and β are the P and S wavespeeds, respectively. Similarly, the isotropic part of the tectonic release can be described in the long-period limit by the scalar moment M_0 given by

$$M_0 = \frac{1}{3} \text{ tr } \underline{\sigma} R^3 \pi \frac{\alpha^2}{\beta^2} \tag{4}$$

However, if we assume that the explosion reduces only the shear strength of the material in the source region, and does not reduce the effective bulk modulus, then the isotropic part of the prestress will not contribute to the seismic radiation.

Using (3), we can derive a simple approximate expression for the ratio of the "tectonic" Rayleigh wave amplitude, A_t, to the explosion, or isotropic, Rayleigh wave amplitude, A_x, which will apply in the long-period limit. For an explosion with isotropic moment M_x and tectonic release components M_{ij}, the ratio A_t/A_x is given by

$$\frac{A_t}{A_x} = \frac{\alpha^2}{2\beta^2 M_x}\left[\frac{1}{2}(M_{11}+M_{22}) - \left(\frac{\alpha^2-2\beta^2}{\alpha^2}\right) M_{33} + \frac{1}{2}(M_{11}-M_{22})\cos 2\phi + M_{12}\sin\right] \qquad (5)$$

where x_1, x_2, x_3 are a right-handed coordinate system with x_3 vertical, and ϕ is the azimuth of the observation point measured from the x_1 axis toward the x_2 axis. Equation (5) follows from Equation 7.149 of Aki and Richards (1980, page 316), for sources located close to the free surface. We have used the fact that the stress eigenfunctions vanish at the free surface, and can therefore be neglected for wavelengths much greater than the source depth. For the cylindrically symmetric prestress field under consideration in the present study (Figure 3), this expression reduces (using Equation 3) to

$$\frac{A_t}{A_x} = \frac{4\beta^2-3\alpha^2}{9\alpha^2-4\beta^2}\,\frac{10\pi\alpha^2}{3\beta^2}\,\frac{(\sigma_V-\sigma_H)\,R^3}{M_x} \quad , \qquad (6)$$

where σ_v and σ_H are the vertical and horizontal principal stresses, respectively. Assuming that there is no time delay between the explosion and the tectonic release, the two Rayleigh wave contributions are either in phase ($A_t/A_x > 0$) or 180° out of phase ($A_t/A_x < 0$).

We can solve Equation 6 for the equivalent cavity radius R by assigning numerical values to $(\sigma_V-\sigma_H)$, M_x, and A_t/A_x, based on the nonlinear simulations. The stress difference $(\sigma_V-\sigma_H)$ in Case 2 was 15 MPa. Comparing synthetic seismograms

for cases 1 and 2 (Figure 8), we estimate the ratio A_t/A_x as

$$\frac{A_t}{A_x} \approx -.757 \quad \text{[from Figure 8]}.$$

Finally the explosion moment can be estimated from the one-dimensional simulation, using the static value of the RDP, Ψ_∞, together with the relationship $M_x = 4\pi\rho\alpha^2\Psi_\infty$. With $\alpha = 5350$ m/sec, $\rho = 2690$ k_2/m^3, and $\Psi_\infty = 1.6 \times 10^4$ m^3 (see Figure 1), this gives

$$M_x = 1.5 \times 10^6 \text{ Nt-m} \quad \text{[from Figure 1]}.$$

Then we can solve Equation 6 for the equivalent cavity radius R:

$$R \approx 480 \text{ m} . \tag{7}$$

(We have also done this calculation using the exact, frequency-dependent expressions for the displacement and stress eigenfunctions, and find $R \approx 460$ m).

This value of the equivalent cavity radius, 480 m, is nearly as large as the elastic radius of approximately 550 m to 600 m which we inferred for the nonlinear simulations from Figure 5b (for comparison, the Mueller-Murphy scaling laws applied to granite (Mueller and Murphy, 1971; Murphy, 1977) give an elastic radius of 720 meters for a 61 kt explosion). Thus, it appears that the linear theory predicts the effect of tectonic release on Rayleigh waves if the equivalent cavity radius is about 80 to 90 percent of the elastic radius.

The maximum shear stress at shot depth assumed in Case 3 (7.5 MPa) was well below the upper bound implied by Byerlee's law. If we assume that the explosion and tectonic release components of the

source add linearly, then increasing the tectonic shear stress to above 10 MPa would be sufficient to reverse the polarity of the Rayleigh wave. Further nonlinear modeling will be required to test this conjecture.

IV. BODY WAVES

Short-period body wave synthetic seismograms for the two two-dimensional simulations were computed using the same surface-integral method as was used to synthesize the surface waves. Again, we quantify the effects of spall and nonhydrostatic prestress by comparing these to synthetic seismograms computed from the one-dimensional simulation, in which these phenomena are absent.

Table 2 shows the crustal structures which were used to represent the source and receiver geologies. The receiver was at a distance of 4000 km (take-off angle equal to 27°). The mantle response was modeled by using a geometric spreading factor, with the effective R^{-1} equal to 6.4×10^{-5} km^{-1}, which is a reasonable approximation to the mantle response at this distance range (Bache et al., 1980). Anelastic attenuation was approximated using a causal attenuation operator with attenuation factor $e^{-\pi f t^*}$; t^* was assumed to be 0.8 sec. The response of the KS 36000 seismometer (peak response ~ 2.5 Hz) was included in the synthetics.

Figure 9 shows the synthetic short-period waveforms for the one- and two-dimensional simulations. The amplitudes are expressed as body wave magnitudes, as measured from the b phase (i.e., first peak to first trough) and c phase (first trough to second peak) respectively, of the waveform. The magnitude was computed from A, the peak-to-peak instrument-corrected amplitude in millimicrons, according to the formula

$$m_b = \log \frac{A}{T} + 3.25,$$

where 3.25 is the distance correction and T is the period of the measured phase.

Comparing the three models, we find that the b phases are virtually identical in waveform and amplitude. Neither spall nor tectonic stress significantly altered m_b measured from the b phase, denoted m_b^b in the figure.

TABLE 2

CRUSTAL STRUCTURES USED TO COMPUTE

BODY-WAVE SYNTHETIC SEISMOGRAMS

Source Region

Thickness (m)	α (m/sec)	β (m/sec)	ρ (kg/m^3)
52	1438	752	2650
96	4600	2795	2650
5030	5352	2795	2650
	6000	3500	2700

Receiver Region

Thickness (km)	α (m/sec)	β (m/sec)	ρ (kg/m^3)
1700	4000	2310	2300
1300	5100	2940	2500
	6000	3500	2800

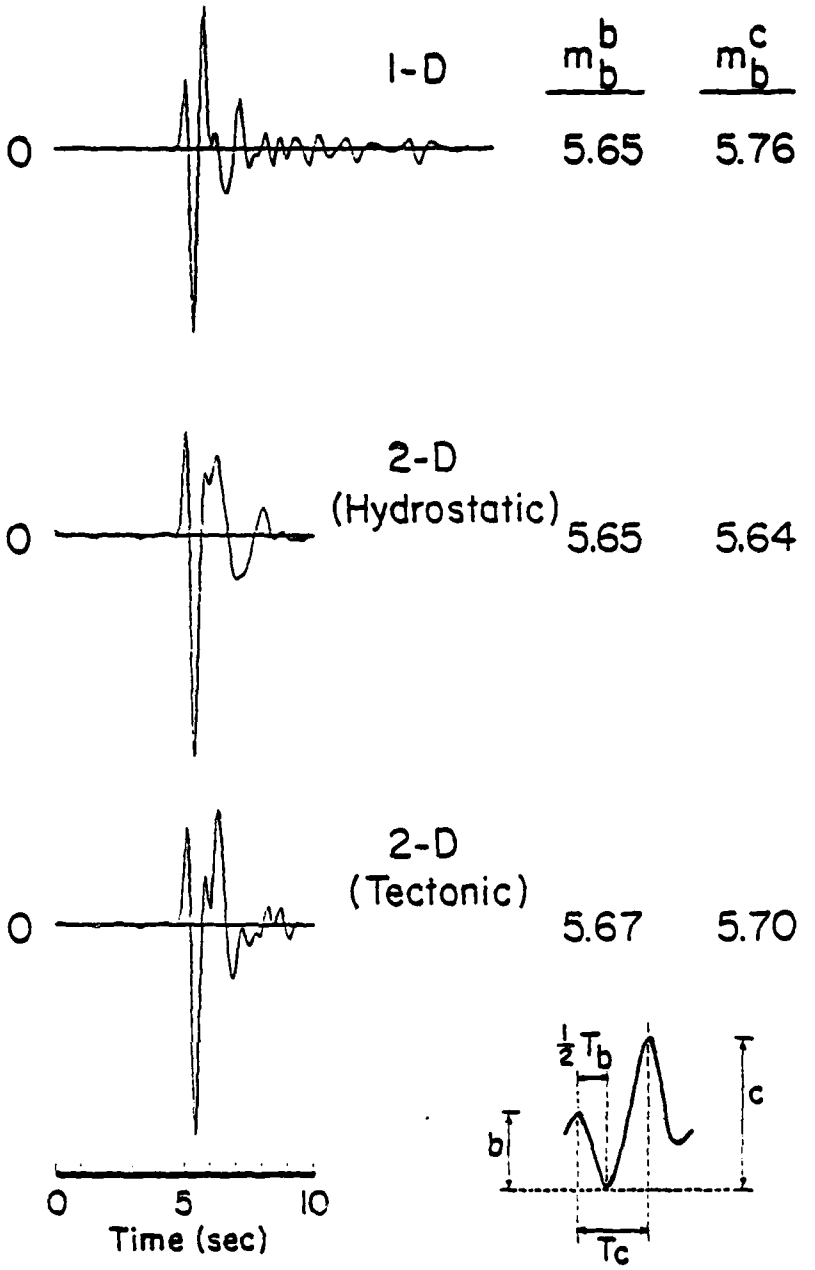

Figure 9. Short-period body wave synthetic seismograms for the one- and two-dimensional simulations. The amplitudes are given on the right in the form of body wave magnitudes m_b^b and m_b^c, measured from the amplitude and period of the "b" and "c" phases, respectively.

The remainder of the short-period waveform is significantly affected by the source physics, however. Most significantly, the second peak is smaller for both two-dimensional models than for the one-dimensional model. The suppression of the second peak is primarily the result of spall (which occurs in both two-dimensional models but cannot occur in the one-dimensional model).

The main effect of spall on the waveforms in Figure 9 can be interpreted as a partial suppression of the short-period components of the reflected phase $_pP$. Similar inferences were drawn, respectively, by Bache et al. (1980) from analogous theoretical calculations, as well as by Bache, Day and Savino (1979) and Murphy, Shah and Tzeng (1982) from analysis of teleseismic data.

Despite this apparent effect on $_pP$, spall only reduced m_b^c by 0.12 (comparing the one- and two-dimensional hydrostatic models). We are reluctant to draw any general conclusions about the effect of spall on short-period waves, however, from calculations performed for only a single source depth. The result is likely to be heavily dependent on source depth, because source depth will affect both the amount and duration of spall as well as the relative timing of P, $_pP$ and the spall slapdown pulse.

More important for our present purposes is the comparison between the two-dimensional hydrostatic and tectonic models. Although there are marked differences in waveform between the two models, there is no significant difference in either m_b^b or m_b^c. Recall that M_s for the tectonic model was suppressed by 0.6 units compared with the hydrostatic model. Thus, it appears that tectonic prestress can cause a very large perturbation to M_s accompanied by virtually no perturbation to m_b. We see no reason to expect this result to be particularly sensitive to source depth.

This result was obtained for the case of a uniform shear field. Stevens (1982) has shown that if much higher, but localized, stress concentrations exist, they can significantly perturb m_b.

V. SUMMARY

The nonlinear models of underground explosions studied here predict that tectonic prestress can strongly perturb the amplitude of radiated surface waves. The tectonic stress field considered here (horizontal principal stresses 15 MPa more compressive than vertical principal stress -- maximum shear stress equal to 7.5 MPa) led to a 4 fold reduction in surface wave amplitudes, compared with hydrostatic initial conditions. If the surface wave perturbation due to tectonic release can be scaled approximately linearly with prestress level, then an initial shear stress exceeding about 10 MPa may be sufficient to reverse the Rayleigh wave polarity. Tectonic release is therefore a potential explanation for observations of reverse-polarity Rayleigh waves, such as those reported for some eastern Kazakh explosions (e.g., Rygg, 1979; Patton, 1980; Cleary, 1981). Further nonlinear simulations at higher shear stress levels are required to test this hypothesis

The nonlinear model calculations indicate that the equivalent cavity radius required by linear theories of tectonic release should be about 80 percent of the explosion elastic radius. That is, the explosion nonlinear volume responds to the deviatoric part of the prestress field approximately as though it were a zero-strength sphere with a radius 80 percent as large as the explosion elastic radius. Again, additional nonlinear simulations are necessary to verify that this result holds for higher values of the tectonic stresses.

Finally, although our nonlinear simulations predict that tectonic release can greatly reduce M_s, this predicted M_s reduction is not accompanied by a significant perturbation to m_b. The analysis of Stevens (1982) shows that this relative insensitivity of m_b to prestress is a general result for smoothly varying prestress fields, although if very high, localized stress concentrations exist at shallow depth, they can significantly perturb m_b.

VI. REFERENCES

Aki, K. and P. G. Richards (1979), Quantitative Seismology — Theory and Methods, W. H. Freeman and Company, San Francisco.

Aki, K. and Y. Tsai (1972), "The Mechanism of Love Wave Excitation by Explosive Sources," J. Geophys. Res., 77, 1452-1475.

Archambeau, C. B. (1972), "The Theory of Stress Wave Radiation from Explosions in Prestressed Media," Geophys. J., 29, 329-366.

Archambeau, C. B. and C. Sammis (1970), "Seismic Radiation from Explosions in Prestressed Media and the Measurement of Tectonic Stress in the Earth," Rev. Geophys., 8, 473-499.

Bache, T. C., J. T. Cherry, N. Rimer, J. M. Savino, T. R. Blake, T. G. Barker, and D. G. Lambert (1975), "An Explanation of the Relative Amplitudes Generated by Explosions in Different Test Areas at NTS," Systems, Science and Software Final Report, submitted to the Defense Nuclear Agency, DNA 3958F, October.

Bache, T. C., S. M. Day, and H. J. Swanger (1982), "Rayleigh Wave Synthetic Seismograms from Multi-Dimensional Simulations of Underground Explosions," Bull. Seism. Soc. Am., 72, 15-28.

Bache, T. C., T. G. Barker, N. Rimer and J. T. Cherry (1980), "The Contribution of Two-Dimensional Source Effects to the Far-Field Seismic Signatures of Underground Nuclear Explosions," Systems, Science and Software Topical Report to Advanced Research Projects Agency, SSS-R-80-4569, July.

Brace, W. F., and D. L. Kohlstedt (1980), "Limits on Lithospheric Stress Imposed by Laboratory Experiments," J. Geophys. Res., 85, 6248-6252.

Burridge, R. and L. Knopoff (1964), "Body Force Equivalents for Seismic Dislocations," Bull. Seism. Soc. Amer., 54, 1875-1888.

Byerlee, J. D. (1968), "Brittle-Ductile Transition in Rocks," J. Geophys. Res., 73, 4741-4750.

Byerlee, J. D. (1978), "Friction of Rocks," Pure Appl. Geophys., 116, 615-626.

Cherry, J. T., N. Rimer and W. O. Wray (1975), "Seismic Coupling from a Nuclear Explosion: The Dependence of the Reduced Displacement Potential on the Nonlinear Behavior of the Near Source Rock Environment," Systems, Science and Software Report submitted to the Advanced Research Projects Agency, SSS-R-76-2742, September.

Cleary, J. R. (1981), "Anomalous Rayleigh Waves from Presumed Explosions in East Kazakh," in Identification of Seismic Sources - Earthquake or Underground Explosion, E. S. Husebye and S. Mykkeltveit (eds), D. Reidel Publishing Company, Dordrecht, Holland.

Day, S. M., N. Rimer and J. T. Cherry (1982), "Surface Waves from Underground Explosions with Spall: Analysis of Elastic and Nonlinear Source Models," submitted to Bull. Seism. Soc. Am.

Harkrider, D. G. (1981), "Coupling Near-Source Phenomena into Surface Wave Generation," in Identification of Seismic Sources - Earthquake or Underground Explosion," E. S. Husebye and S. Mykkeltveit, Editors, D. Reidel Publishing Co., Dordrecht, Holland.

Hoffman, H. V. and F. M. Sauer (1969), "Free Field and Surface Motions, PILEDRIVER Event," Stanford Research Institute Report, POR-4000.

Jaeger, J. C., and N. G. W. Cook (1976), "Fundamentals of Rock Mechanics," John Wiley, New York, 585.

Masse, R. P. (1981), "Review of Seismic Source Models for Underground Nuclear Explosions," Bull. Seism. Soc. Am., 71, 1249-1268.

McGarr, A., and N. C. Gay (1978), "State of Stress in the Earth's Crust," Annu. Rev. Earth Planet Scie., 6.

Minster, J. B. (1973), "Elastodynamics of Failure in a Continuum," Ph.D. Thesis, California Institute of Technology, Pasadena, California.

Mueller, R. A. and J. R. Murphy (1971), "Seismic Characteristics of Underground Nuclear Detonations: Part 1., Seismic Scaling Law of Underground Detonations," Bull. Seism. Soc. Am., 61, 1675-1692.

Murphy, J. R. (1977), "Seismic Source Functions and Magnitude Determinations for Underground, Nuclear Detonations," Bull. Seism. Soc. Am., 67, 135-158.

Murphy, J. R. , H. K. Shah, and T. K. Tzeng (1982), "Magnitude/Yield Variability in the Western United States: Analysis of Gasbuggy Regional and Teleseismic Data," S-CUBED Semiannual Report submitted to Air Force Office of Scientific Research, SSS-R-82-5643, July 1982.

Patton, H. J. (1980), "Surface-Wave Generation by Underground Nuclear Explosions Releasing Tectonic Strain," Lawrence Livermore Laboratory Report UCRL-53062.

Press, F. and C. B. Archambeau (1962), "Release of Tectonic Strain by Underground Explosions," J. Geophys. Res., 67, 337-343.

Rimer, N., J. T. Cherry, S. M. Day, T. C. Bache, J. R. Murphy and A. Maewal (1979), "Two-Dimensional Calculation of PILEDRIVER, Analytic Continuation of Finite Difference Source Calculations, Analysis of Free Field Data from MERLIN and Summary of Current Research," Systems, Science and Software Quarterly Technical Report submitted to VSC/ARPA, SSS-R-79-4121, August.

Rygg, E. (1979), "Anomalous Surface Waves from Underground Explosions," Bull. Seism. Soc. Am., 69, 1995-2002.

Stevens, J. L. (1980a), "Seismic Radiation from the Sudden Creation of a Spherical Cavity in an Arbitrarily Prestressed Elastic Medium," Geophys. J. R. astr. Soc., 61, 303-328.

Stevens, J. L. (1980b), "Seismic Stress Relaxation Phenomena in an Inhomogeneously Prestressed Medium," Ph.D. Thesis, University of Colorado, Boulder, Colorado.

Stevens, J. L. (1982), "A Model for Tectonic Release from Explosions in Complex Prestress Fields Applied to Anomalous Seismic Waves from NTS and Eastern Kazakh Explosions," S-CUBED Report submitted to Advanced Research Projects Agency, SSS-R-82-5358, January 1982.

Toksoz, M. N. and H. H. Kehrer (1971), "Underground Nuclear Explosions: Tectonic Utility and Dangers," Science, 173, 230-233.

Zoback, M. D., H. Tsukahara, and S. Hickman (1980), "Stress Measurements at Depth in the Vicinity of the San Andreas Fault: Implications for the Magnitude of Shear Stress at Depth," J. Geophys. Res., 85, 6157-6173.

APPENDIX

MOMENT TENSOR OF A RELAXATION SOURCE

Expressions for the moment tensor components of a relaxation source can be obtained by comparing the static solution for a spherical cavity in a prestressed medium with the static solution for a dislocation source. The static displacement field in the radial direction due to a dislocation source with non-zero moment tensor components M_{13} and M_{31}, is given by (Aki and Richards, 1980)

$$U_r = \frac{M_{13}}{8\pi\rho\, r^2} \left(\frac{3\alpha^2 - \beta^2}{\alpha^2\, \beta^2} \right) \sin 2\theta \cos\phi \qquad \text{(A1)}$$

where r, θ, and ϕ are spherical coordinates and α, β, ρ are the compressional velocity, shear velocity and density.

For a relaxation source, there are, in general, terms in the static displacement field which fall off faster than r^{-2}. In the initial value-formulation of the dynamic relaxation source (Stevens, 1980b), these higher order terms do not contribute to the long-period radiation and do not contribute to the seismic moment. For a stress field with only σ_{13} and σ_{31} components, neglecting higher order terms, the radial component of the displacement field is given by

$$u_r = \frac{\sigma_{13}\, R^3}{\rho\, r^2} \sin 2\theta \cos\phi \left(\frac{5(3\alpha^2 - \beta^2)}{36\, \alpha^2\beta^2 - 16\, \beta^4} \right) . \qquad \text{(A2)}$$

Comparing (A1) with (A2) we have

$$M_{13} = \sigma_{13}\, R^3\, \frac{20\pi\, \alpha^2}{9\alpha^2 - 4\beta^2} .$$

In general, for an arbitrary orientation of a pure shear (trace $\underset{\approx}{\sigma} = 0$) stress field

$$M_{ij} = \sigma_{ij} R^3 \frac{20\pi \alpha^2}{9\alpha^2 - 4\beta^2} \quad . \tag{A3}$$